INSTITUTE OF MATHEMATICS

THE CZECH ACADEMY OF SCIENCES

Convergent numerical method for the Navier-Stokes-Fourier system: a stabilized scheme

Radim Hošek
Bangwei She

Preprint No. 70-2017

PRAHA 2017

Convergent numerical method for the Navier-Stokes-Fourier system: a stabilized scheme

Radim Hošek, Bangwei She*

Insitute of Mathematics, Czech Academy of Sciences,
Zitna 25, 11567, Prague, Czech Republic

Abstract

We propose a combined finite volume-finite element method for the compressible Navier-Stokes-Fourier system. A finite volume approximation is used for the density and energy equations while a finite element discretization based on the non-conforming Crouzeix-Raviart element is applied to the momentum equation. We show the stability, the consistency and finally the convergence of the scheme to a sequence of suitable weak solution. We are interested in the case that the velocity diffusion in the momentum equation is presented by the divergence of the symmetric velocity gradient instead of the classical Laplace form. As a consequence, there emerges the need to add a stabilization term that substitutes the role of Korn's inequality which does not hold in the Crouzeix–Raviart element space. Moreover, we present the numerical performance of the scheme as well as that of [15], where a similar result is theoretically studied for the case of using the Laplace type diffusion and the numerical performance is expected here.

keywords Navier-Stokes-Fourier, finite element method, finite volume method, Korn inequality, convergence, stability

1 Introduction

We are interested in the Navier-Stokes-Fourier system which describes a compressible viscous and heat conducting flow in a bounded domain $\Omega \subset \mathcal{R}^d, d = 2, 3$.

$$\rho_t + \nabla \cdot (\rho \mathbf{u}) = 0. \tag{1a}$$

$$(\rho \mathbf{u})_t + \mathrm{div}(\rho \mathbf{u} \otimes \mathbf{u}) = -\nabla p + \mathrm{div}\mathbb{S}(\nabla \mathbf{u}). \tag{1b}$$

$$c_v\big((\rho\theta)_t + \mathrm{div}(\rho\theta\mathbf{u})\big) + \mathrm{div}\mathbf{q}(\theta, \nabla\theta) = \mathbb{S}(\nabla\mathbf{u}) : \nabla\mathbf{u} - \theta\frac{\partial p(\rho,\theta)}{\partial\theta}\mathrm{div}\mathbf{u}. \tag{1c}$$

where $\rho, \mathbf{u}, p, \theta$ are the fluid density, velocity, pressure, and temperature, c_v is the specific heat per volume. The viscous stress tensor takes the form

$$\mathbb{S} = 2\mu\mathbf{D}(\mathbf{u}) + \nu\mathrm{div}\mathbf{u}\mathbb{I} \text{ and } \mu \geq 0, 2\mu + d\nu \geq 0, \mathbf{D}(\mathbf{u}) = \frac{1}{2}\left(\nabla\mathbf{u} + \nabla\mathbf{u}^T\right).$$

*The research of the authors leading to these results has received funding from the European Research Council under the European Unions Seventh Framework Programme (FP7/2007-2013)/ ERC Grant Agreement 320078. The Institute of Mathematics of the Academy of Sciences of the Czech Republic is supported by RVO:67985840.

The heat flux $\mathbf{q}$ obeys Fourier's law

$$\mathbf{q} = -\nabla \mathcal{K}(\theta), \mathcal{K}(\theta) = \int_0^\theta \kappa(z)dz, \text{ with } \underline{\kappa}(1+\theta^2) \leq \kappa(\theta) \leq \bar{\kappa}(1+\theta^2), \underline{\kappa} > 0.$$

We take a general equation of state

$$p = a\rho^\gamma + b\rho + \rho\theta,\ a, b > 0,\ \gamma > 3, \text{ and } \frac{\partial p(\rho,\theta)}{\partial \theta} = \rho.$$

To close the system we apply the no-slip boundary condition

$$\mathbf{u}|_{\partial\Omega} = 0, \tag{1d}$$

and the following initial conditions

$$\rho(\mathbf{x}, 0) = \rho_0 > 0, \quad \mathbf{u}(\mathbf{x}, 0) = \mathbf{u}_0, \quad \theta(\mathbf{x}, 0) = \theta_0 > 0. \tag{1e}$$

The existence of global in time weak solutions to this compressible Navier-Stokes system was established in [10], and a weak strong uniqueness result can be found in [16].

Here we adopt the weak formulation introduce in [10, Chapter 4] and present everything for $d = 3$, bearing in mind that for $d = 2$ even a better result can be deduced due to better Sobolev embeddings.

Definition 1. *We say that a trio of functions $[\rho, \mathbf{u}, \theta]$ is a weak solution to the problem (1) in $(0,T)\times\Omega$ if:*

$$\rho \in L^\infty(0,T; L^\gamma(\Omega)), \mathbf{u} \in L^2(0,T; W_0^{1,2}(\Omega; R^3)), \theta \in L^2(0,T; L^6(\Omega)), \tag{2a}$$

$$\rho\mathbf{u} \in L^\infty(0,T; L^{\frac{2\gamma}{\gamma+1}}(\Omega; R^3)), \rho\theta \in L^\infty(0,T; L^1(\Omega)); \tag{2b}$$

$$\rho \geq 0,\ \theta > 0 \ \textit{a.a. in } (0,T)\times\Omega; \tag{2c}$$

$$\int_0^T \int_\Omega [\rho\partial_t\psi + \rho\mathbf{u}\cdot\nabla\psi]\, dxdt = -\int_\Omega \rho_0\psi(0,\cdot)dx, \quad \forall\, \psi \in C_c^\infty([0,T)\times\bar{\Omega}); \tag{2d}$$

$$\int_0^T \int_\Omega [\rho\mathbf{u}\partial_t\psi + \rho\mathbf{u}\otimes\mathbf{u} : \nabla\psi + p(\rho,\theta)div\psi + 2\mu\mathbf{D}(\mathbf{u}) : \mathbf{D}(\psi) + \nu div\mathbf{u} div\psi]\, dxdt$$
$$= -\int_\Omega \rho_0\mathbf{u}_0\psi(0,\cdot)dx, \quad \forall\psi \in C_c^\infty([0,T)\times\Omega; R^3); \tag{2e}$$

$$\int_0^T \int_\Omega \left[c_v(\rho\theta\partial_t\psi + \rho\theta\mathbf{u}\cdot\nabla\psi - \mathcal{K}(\theta)\Delta\psi + 2\mu|\mathbf{D}(\mathbf{u})|^2\psi + \nu|div\mathbf{u}|^2\psi\right] dxdt$$
$$- \int_0^T \int_\Omega \rho\theta div\mathbf{u}\psi dxdt \leq -\int_\Omega c_v\rho_0\theta_0\psi(0,\cdot)dx, \quad \forall\,\psi \geq 0,\ \psi \in C_c^\infty([0,T)\times\bar{\Omega}) \tag{2f}$$

where $\nabla\psi\cdot\mathbf{n}|_{\partial\Omega} = 0$;

$$\int_\Omega \left[\frac{1}{2}\rho|\mathbf{u}|^2 + c_v\rho\theta + \frac{a}{\gamma-1}\rho^\gamma + b\rho\log(\rho)\right](\tau,\cdot)dx$$
$$\leq \int_\Omega [\frac{1}{2}\rho_0|\mathbf{u}_0|^2 + c_v\rho_0\theta_0 + \frac{a}{\gamma-1}\rho_0^\gamma + b\rho_0\log(\rho_0)]dx \textit{ for a.a. } \tau \in (0,T). \tag{2g}$$

Numerical study of this model has attracted huge interests. Let us mention a few of them, for example, finite volume method [5, 20], finite element method [23, 27], discontinuous Galerkin method [7, 26, 30, 31, 35], mixed finite volume-finite element method on non-conforming Crouzeix-Raviart elements [11, 13, 15], kinetic BGK scheme [36]. See also some other schemes [6, 19, 28, 32].

Despite a large variety of numerical schemes available in the literature, their convergence to the physical solution is rather underdeveloped. Our main goal follows in this direction to achieve a convergent scheme for the Navier-Stokes-Fourier system. The designed scheme is a mixed finite volume-finite element(FV-FE) method, motivated from a combination of the methods proposed by Eymard et. al. [8, 9] and by Karper [25]. On one hand, the former proved the convergence of a finite volume scheme for the convection-diffusion equation. On the other hand, the latter showed the convergence of a low-order FEM-DG method based on the non-conforming Crouzeix-Raviart element for the compressible Navier-Stokes, see also [12, 14] for its extension to smooth and general domain.

This paper is an extension of Feireisl et al. [15], where the convergence of a FV-FE scheme to the Navier-Stokes-Fourier system has been studied theoretically, while the numerical performance is expected in this paper. The work [15] was also extended for a flow in a smooth domain where the numerical scheme is defined on a family of polyhedral domains, converging to the target one only in the sense of compacts, see [13]. Our work could be also rephrased as an extension of [13], without any additional difficulties. Here we decided to stick to [15] mainly due to the numerical tests taking place in a polyhedral domain.

Our first aim is to follow [15] and show the convergence of our new scheme theoretically. The difference here is that we would like to consider a more physical dissipation mechanism in the temperature energy balance law

$$\Phi = 2\mu|\mathbf{D}(\mathbf{u})|^2 + \nu|\mathrm{div}\mathbf{u}|^2$$

instead of $\Phi = \mu|\nabla\mathbf{u}|^2+\lambda|\mathrm{div}\mathbf{u}|^2$ considered in the paper [15] for $\lambda = \mu+\nu$. These two terms are not equal when a finite volume scheme is applied to the balance law of energy, see Remark 2. For this reason we want to use $|\mathbf{D}(\mathbf{u})|^2$ instead of $|\nabla\mathbf{u}|^2$ in our finite volume approximation of the energy equation. Moreover, we will use $\int_\Omega \mathbf{D}(\mathbf{u})\mathbf{D}(\mathbf{v})$ instead of $\int_\Omega \nabla\mathbf{u}\nabla\mathbf{v}$ in the finite element approximation of the momentum equation. Then the issue occurs that the Korn inequality is not admissible for the non-conforming Crouzeix-Raviart element used in our scheme. Thus we introduce a stabilization term studied by [3, 17, 21] and aim to show the convergence of the stabilized scheme to suitable weak solution.

Another aim of this paper is to show the numerical performance of the scheme studied in [15] as well as the stabilized scheme proposed here.

The rest of the paper is organized as follows. In Section 2 we give the notations and prescribe the scheme as well as the main result. Sections 3 is devoted to the proof of the main result through stating the stability, consistency and finally the convergence. In the last section, we perform some numerical experiments of the schemes.

2 Numerical scheme

2.1 Time discretization

Let us extend for convenience the numerical solution to be defined for any $t \in [0,T]$ as follows

$$\rho_h(t,\cdot) = \rho_h^k,\ \theta_h(t,\cdot) = \theta_h^k,\ \mathbf{u}_h(t,\cdot) = \mathbf{u}_h^k,\ \text{ for } t \in [k\Delta t,(k+1)\Delta t),\ k = 1,2,\cdots,N_T = \frac{T}{\Delta t} \text{ and}$$

$$\rho_h(t,\cdot) = \rho_h^0,\ \theta_h(t,\cdot) = \theta_h^0,\ \mathbf{u}_h(t,\cdot) = \mathbf{u}_h^0,\ \text{ for } t \le 0.$$

Accordingly, we set the discrete time derivative of a quantity v_h as

$$D_t v_h(t,\cdot) = \frac{v_h(t) - v_h(t-\Delta t)}{\Delta t},\ t > 0.$$

2.2 Space discretization

Let the physical domain Ω be polyhedral, divided into triangulation $\mathcal{T}_h$, $\mathcal{E}$ be the collection of all $(d-1)$-dimensional faces, $\mathcal{E}_{ext} = \mathcal{E} \cap \partial\Omega$ be the exterior faces, $\mathcal{E}_{int} = \mathcal{E} \setminus \mathcal{E}_{ext}$ be the interior faces, $K \in \mathcal{T}_h$ be an arbitrary element. In addition, we require the mesh $\mathcal{T}_h$ to be in the sense of Eymard et al. [9]:

- for $K, L \in \mathcal{T}_h, K \neq L$, the intersection $K \cap L$ is either a vertex, or an edge, or a face $\Gamma \in \mathcal{E}$.
- There is a family of control points $\{\mathbf{x}_K | \mathbf{x}_K \in K, K \in \mathcal{T}_h\}$ such that the segment $[\mathbf{x}_K, \mathbf{x}_L]$ for two adjacent elements K, L is perpendicular to their common face $\Gamma = K \cap L$. We denote their distance as $d_\Gamma \equiv |\mathbf{x}_K - \mathbf{x}_L|$.
- The mesh is regular in the sense that $\inf\limits_{K\in\mathcal{T}_h} \inf\limits_{\Gamma\in\partial K} \mathrm{dist}[\mathbf{x}_K, \Gamma] \gtrsim h$.

Remark 1. *The above properties are satisfied, for example, by the well-centered meshes studied by VanderZee et al. [33, 34], where the control points are simply the circumcenters of the elements.*

Let $\Gamma = K \cap L$ be an edge of element K, $\mathbf{n}_{\Gamma,K}$ be its outer normal pointing from K to L. Then for piecewise constant f we can define the jump and average operators on the face Γ

$$[\![f]\!]_\Gamma = f_L - f_K, \quad \{f\}_\Gamma = \frac{1}{2}(f_K + f_L). \tag{3}$$

and upwind flux

$$\mathcal{F}(f,\mathbf{u})|_\Gamma = f_K[s_{\Gamma,K}]^+ + f_L[s_{\Gamma,K}]^- = \begin{cases} f_K\, s_{\Gamma,K} & \text{if } s_{\Gamma,K} \geq 0, \\ f_L\, s_{\Gamma,K} & \text{else.} \end{cases} \tag{4}$$

where we have denoted

$$[c]^+ = \max\{0, c\}, \quad [c]^- = \min\{0, c\}, \quad s_{\Gamma,K} = \tilde{\mathbf{u}} \cdot \mathbf{n}_{\Gamma,K}, \quad \tilde{\mathbf{u}} = \frac{1}{|\Gamma|}\int_\Gamma \mathbf{u} d\sigma.$$

Further, the average operator on the element K is given by

$$\hat{f}_K = \frac{1}{|K|}\int_K f dx. \tag{5}$$

We also denote

$$\mathrm{co}\{a, b\} = [\min(a,b), \max(a,b)]\,.$$

2.2.1 Functional spaces

Specifically, we adopt the piecewise linear Crouzeix-Raviart elements for the discretization of velocity, while the density and pressure are set as piecewise constants. The functional spaces are defined as

$$\begin{aligned}
&Q_h \equiv \{\phi_h \in L^2(\Omega); \phi_h|_K \in \mathcal{P}^0(K), K \in \mathcal{T}_h\}, \\
&V_h \equiv \{\mathbf{v}_h \in L^2(\Omega); \mathbf{v}_h|_K \in \mathcal{P}^1(K), \forall K \in \mathcal{T}_h; \int_\Gamma [\![\mathbf{v}_h]\!] = 0, \forall\ \Gamma \in \mathcal{E}_{int}\}, \\
&V_{0,h} \equiv \{\mathbf{v}_h \in V_h(\Omega); \int_\Gamma \mathbf{v}_h = 0, \forall\ \Gamma \in \mathcal{E}_{ext}\},
\end{aligned}$$

where $\mathcal{P}^n(K)$ denotes polynomial of degree not greater than n on element K.

2.2.2 Discrete Sobolev spaces

In the following we introduce the associated projections to the functional spaces

$$\Pi_h^Q \ : \ L^2(\Omega) \mapsto Q_h, \quad \Pi_h^V \ : \ W^{1,1}(\Omega) \mapsto V_h,$$

defined by

$$\Pi_h^Q[\phi]|_K = \hat{\phi}_K, \forall\, K \in \mathcal{T}_h; \quad \int_\Gamma \Pi_h^V[\mathbf{v}] = \int_\Gamma \mathbf{v}, \forall\, \Gamma \in \mathcal{E}. \tag{6}$$

Then it is easy to observe the following properties, see also similar result in [25, Lemma 2.11]

$$\mathrm{div}_h \Pi_h^V[\mathbf{v}] = \Pi_h^Q[\mathrm{div}\mathbf{v}], \quad \int_\Omega \mathbf{D}_h(\mathbf{u}_h) : \mathbf{D}_h(\Pi_h^V[\mathbf{v}] - \mathbf{v}) = 0, \text{ for } \mathbf{u}_h \in V_h, \mathbf{v} \in W^{1,1}. \tag{7}$$

For $\phi \in Q_h, \mathbf{v} \in V_{0,h}$, let us denote the following norms

$$\|\phi\|^2_{H^1_{Q_h}(\mathcal{E})} := \sum_{\Gamma\in\mathcal{E}_{int}} \int_\Gamma \frac{1}{h} [\![\phi]\!]^2 d\sigma, \qquad \|\mathbf{v}\|^2_{H^1_{V_h}(\mathcal{E})} := \sum_{\Gamma\in\mathcal{E}_{int}} \int_\Gamma \frac{1}{h} [\![\mathbf{v}]\!]^2 d\sigma,$$
$$\|\mathbf{v}\|^2_{H^1} := \sum_{K\in\mathcal{T}_h} \int_K |\mathbf{D}(\mathbf{v})|^2 dx + \sum_{\Gamma\in\mathcal{E}_{int}} \int_\Gamma \frac{1}{h} [\![\mathbf{v}]\!]^2 d\sigma = \|\mathbf{D}(\mathbf{v})\|^2_{L^2} + \|\mathbf{v}\|^2_{H^1_{V_h}(\mathcal{E})}.$$

Then we have the following inequality, see [18, Lemma 2.2].

$$\|\mathbf{v}\|_{H^1_{V_h}(\mathcal{E})} \lesssim \|\nabla_h \mathbf{v}\|_{L^2}, \forall\, \mathbf{v} \in V_h \tag{8}$$

and with elementwise application of Sobolev inequality also

$$\|\mathbf{v}\|_{L^6} \lesssim \|\nabla_h \mathbf{v}\|_{L^2}, \ \forall \mathbf{v} \in V_{0,h}. \tag{9}$$

Further, the interpolation error estimates can be stated as

$$\|\phi - \Pi_h^B[\phi]\|_{L^\infty} \le h \|\nabla_x \phi\|_{L^\infty}, \tag{10}$$
$$\|\mathbf{v} - \Pi_h^V[\mathbf{v}]\|_{L^2} \le h \|\nabla_x \mathbf{v}\|_{L^2}, \tag{11}$$

Following the proof of [18, Lemma 2.2], using the continuity of $\mathbf{v}$ across the edge and [25, Lemma 2.7], we can derive

$$\|[\![\Pi_h^V[\mathbf{v}]]\!]\|_{H^1_{V_h}(\mathcal{E})} = \left(\sum_{\Gamma\in\mathcal{E}_{int}} \int_\Gamma \frac{1}{h} [\![\Pi_h^V[\mathbf{v}] - \mathbf{v}]\!]^2 d\sigma \right)^{\frac{1}{2}} \lesssim h \|\nabla_x^2 \mathbf{v}\|_{L^2}, \tag{12}$$

for $\mathbf{v} \in C^2(\Omega), \mathbf{v}|_{\partial\Omega} = 0$.

Importantly, we need the compensated Korn inequality,

$$\|\mathbf{v}\|^2_{L_2} + \|\nabla_h \mathbf{v}\|^2_{L_2} \lesssim \|\mathbf{v}\|^2_{H^1}, \quad \mathbf{v} \in V_{0,h}, \tag{13}$$

which is a consequence of a work of Brenner. In particular, we combine relation (1.19) in [2], relation (1.3) in [1] and zero Dirichlet boundary condition for $\mathbf{v}$.

After applying the Poincaré inequality we also have

$$\|\nabla_h \mathbf{v}\|^2_{L^2} \lesssim \|\mathbf{v}\|^2_{H^1}, \quad \mathbf{v} \in V_{0,h}. \tag{14}$$

2.3 Scheme

With the notations defined above, we propose the numerical scheme for the Navier-Stokes-Fourier system (1). Hereafter, we will call it as 'SA' while 'SB' for the scheme studied in [15].

Definition 2 (Scheme SA)**.** *Find* $\{(\rho_h^{k+1}, \mathbf{u}_h^{k+1}, \theta_h^{k+1})\}_{k=0}^{N_{T-1}} \subset (Q_h \times V_{0,h} \times Q_h)$ *such that for any* $(\phi_h, \mathbf{v}_h) \in (Q_h \times V_{0,h})$ *we have*

$$\int_K \frac{\rho_h^{k+1} - \rho_h^k}{\Delta t}\phi_h - \sum_{\Gamma\in\partial K}\int_\Gamma \Big(\mathcal{F}(\rho_h^{k+1}, \mathbf{u}_h^{k+1})[\![\phi_h]\!] - h^\alpha [\![\rho_h^{k+1}]\!][\![\phi_h]\!]\Big) = 0, \forall K \in \mathcal{T}_h, \tag{15a}$$

$$\begin{aligned}
&\sum_{K\in\mathcal{T}_h}\int_K \frac{\mathbf{q}_h^{k+1} - \mathbf{q}_h^k}{\Delta t}\mathbf{v}_h - \sum_{K\in\mathcal{T}_h}\sum_{\Gamma\in\partial K}\int_\Gamma \mathcal{F}\big(\mathbf{q}_h^{k+1}, \mathbf{u}_h^{k+1}\big)[\![\hat{\mathbf{v}}_h]\!] \\
&\quad - \sum_{K\in\mathcal{T}_h}\int_K p_h^{k+1} div_h \mathbf{v}_h + 2\mu \sum_{K\in\mathcal{T}_h}\int_K \mathbf{D}_h(\mathbf{u}_h^{k+1}) : \mathbf{D}_h(\mathbf{v}_h) + \nu \sum_{K\in\mathcal{T}_h}\int_K div_h \mathbf{u}_h^{k+1} div_h \mathbf{v}_h \\
&\qquad +2\mu \sum_{K\in\mathcal{T}_h}\sum_{\Gamma\in\partial K}\int_\Gamma \frac{1}{h}[\![\mathbf{u}_h^{k+1}]\!][\![\mathbf{v}_h]\!] + h^\alpha \sum_{K\in\mathcal{T}_h}\sum_{\Gamma\in\partial K}\int_\Gamma [\![\rho_h^{k+1}]\!]\{\hat{\mathbf{u}}_h^{k+1}\}[\![\hat{\mathbf{v}}_h]\!] = 0,
\end{aligned} \tag{15b}$$

$$\begin{aligned}
&c_v \int_K \frac{\Theta_h^{k+1} - \Theta_h^k}{\Delta t}\phi_h + \sum_{\Gamma\in\partial K}\int_\Gamma \frac{1}{d_\Gamma}[\![\mathcal{K}(\theta_h^{k+1})]\!][\![\phi_h]\!] + \int_K \Theta_h^{k+1} div_h \mathbf{u}_h^{k+1}\phi_h \\
&\quad - c_v \sum_{\Gamma\in\partial K}\int_\Gamma \mathcal{F}\big(\Theta_h^{k+1}, \mathbf{u}_h^{k+1}\big)[\![\phi_h]\!] \;=\; \int_K \big(2\mu|\mathbf{D}(\mathbf{u}_h^{k+1})|^2 + \nu|div\mathbf{u}_h^{k+1}|^2\big)\phi_h, \forall K \in \mathcal{T}_h
\end{aligned} \tag{15c}$$

where $\mathbf{q}_h$ *and* Θ_h *are the momentum and the internal energy, which are defined as piecewise constant for all* $K \in \mathcal{T}_h$

$$\mathbf{q}_h|_K = \rho_h \hat{\mathbf{u}}_K, \quad \Theta_h = \rho_h \theta_h \tag{16}$$

and the initial conditions for the scheme are given by

$$\varrho_K^0 = \Pi_h^Q[\varrho_0]|_K, \quad \mathbf{q}_K^0 = \Pi_h^Q[\varrho_0\mathbf{u}_0]|_K, \quad \theta_K^0 = \Pi_h^Q[\theta_0]|_K. \tag{17}$$

Before going further, let us recall the scheme SB presented in [15].

Definition 3. *(Scheme SB [15]) Find* $\{(\rho_h^{k+1}, \mathbf{u}_h^{k+1}, \theta_h^{k+1})\}_{k=0}^{N_{T-1}} \subset (Q_h \times V_{0,h} \times Q_h)$ *such that for any* $(\phi_h, \mathbf{v}_h) \in (Q_h \times V_{0,h})$ *we have*

$$\int_K \frac{\rho_h^{k+1} - \rho_h^k}{\Delta t}\phi_h - \sum_{\Gamma\in\partial K}\int_\Gamma \Big(\mathcal{F}(\rho_h^{k+1}, \mathbf{u}_h^{k+1})[\![\phi_h]\!] - h^\alpha [\![\rho_h^{k+1}]\!][\![\phi_h]\!]\Big) = 0, \forall K \in \mathcal{T}_h \tag{18a}$$

$$\begin{aligned}
&\sum_{K\in\mathcal{T}_h}\int_K \frac{\mathbf{q}_h^{k+1} - \mathbf{q}_h^k}{\Delta t}\mathbf{v}_h - \sum_{K\in\mathcal{T}_h}\sum_{\Gamma\in\partial K}\int_\Gamma \mathcal{F}\big(\mathbf{q}_h^{k+1}, \mathbf{u}_h^{k+1}\big)[\![\hat{\mathbf{v}}_h]\!] \\
&\quad - \sum_{K\in\mathcal{T}_h}\int_K p_h^{k+1} div_h \mathbf{v}_h + \mu \sum_{K\in\mathcal{T}_h}\int_K \nabla_h \mathbf{u}_h^{k+1} : \nabla_h \mathbf{v}_h + \lambda \sum_{K\in\mathcal{T}_h}\int_K div_h \mathbf{u}_h^{k+1} div_h \mathbf{v}_h \\
&\qquad + h^\alpha \sum_{K\in\mathcal{T}_h}\sum_{\Gamma\in\partial K}\int_\Gamma [\![\rho_h^{k+1}]\!]\{\hat{\mathbf{u}}_h^{k+1}\}[\![\hat{\mathbf{v}}_h]\!] = 0,
\end{aligned} \tag{18b}$$

$$c_v \int_K \frac{\Theta_h^{k+1}-\Theta_h^k}{\Delta t}\phi_h + \sum_{\Gamma\in\partial K}\int_\Gamma \frac{1}{d_\Gamma}[\![\mathcal{K}(\theta_h^{k+1})]\!][\![\phi_h]\!] + \int_K \Theta_h^{k+1} div_h \mathbf{u}_h^{k+1}\phi_h$$
$$- c_v \sum_{\Gamma\in\partial K}\int_\Gamma \mathcal{F}\big(\Theta_h^{k+1},\mathbf{u}_h^{k+1}\big)[\![\phi_h]\!] = \underline{\int_K \big(\mu|\nabla_h \mathbf{u}_h^{k+1}|^2 + \lambda|div\mathbf{u}_h^{k+1}|^2\big)\phi_h}, \forall K\in\mathcal{T}_h, \quad (18c)$$

and (16) and (17).

Remark 2. *Comparing the schemes SA (15) and SB (18), the only differences are the diffusion terms, marked by underline. As mentioned in the introduction, we have the following equality in the finite element method, supplied with no-slip boundary condition* $\mathbf{u}|_{\partial\Omega}=0$,

$$\int_\Omega 2\mu\mathbf{D}_h(\mathbf{u}_h^{k+1}):\mathbf{D}_h(\mathbf{v}_h) + \nu div_h\mathbf{u}_h^{k+1} div_h\mathbf{v}_h = \int_\Omega \mu\nabla_h\mathbf{u}_h^{k+1}:\nabla_h\mathbf{v}_h + \lambda div_h\mathbf{u}_h^{k+1} div_h\mathbf{v}_h.$$

However, we lose such equality in the finite volume method when the integral is specified on an arbitrary element $K\in\mathcal{T}_h$

$$\int_K 2\mu\mathbf{D}_h(\mathbf{u}_h^{k+1}):\mathbf{D}_h(\mathbf{v}_h) + \nu div_h\mathbf{u}_h^{k+1} div_h\mathbf{v}_h \neq \int_K \mu\nabla_h\mathbf{u}_h^{k+1}:\nabla_h\mathbf{v}_h + \lambda div_h\mathbf{u}_h^{k+1} div_h\mathbf{v}_h.$$

Clearly, the diffusion terms in (15c) are more physically reasonable than that in (18c).

2.4 Main result

Our main result is stated as follows:

Theorem 1. *Let* $\Omega\subset R^3$ *be a bounded polyhedral domain admitting a tetrahedral mesh satisfying assumptions described in Section 2.2 for any* $h>0$. *Let* $[\rho_h,\mathbf{u}_h,\theta_h]$ *be a family of numerical solutions constructed by the scheme (15) such that*

$$\rho_h,\theta_h>0 \text{ for all } h>0, \text{ with } \Delta t\approx h,\ \gamma>3.$$

Then, at least for a suitable subsequence,

$$\rho_h\to\rho \text{ weakly-(*) in } L^\infty(0,T;L^\gamma(\Omega)) \text{ and strongly in } L^1((0,T)\times\Omega),$$
$$\theta_h\to\theta \text{ weakly in } L^2(0,T;L^2(\Omega)),$$
$$\mathbf{u}_h\to\mathbf{u} \text{ weakly in } L^2(0,T;L^6(\Omega;R^3)), \nabla_h\mathbf{u}_h\to\nabla\mathbf{u} \text{ weakly in } L^2((0,T)\times\Omega;R^{3\times3})$$

where $[\rho,\mathbf{u},\theta]$ *is a weak solution of the problem (1) in the sense of Definition 1.*

Remark 3. *The theorem holds also for* $d=2$. *Moreover, the condition of* $\gamma>3$ *will be more lax due to better Sobolev embeddings which we leave it as an exercise to the readers.*

3 Proof of main result Theorem 1

This section is devoted to the proof of the main result Theorem 1. As this paper is an extension of [15], we will only show the proof for the parts that are different. In what follows, we will give the proof by showing the stability, consistency and convergence step by step.

3.1 Renormalization

In this subsection, we introduce two renormalized equations and total energy balance from [15, Section 4].

Lemma 1. *[15, Section 4.1](Renormalized continuity)*

$$\int_{\mathcal{T}_h} D_t B(\rho_h^k)\phi dx - \sum_{\Gamma\in\mathcal{E}_{int}}\int_\Gamma \mathcal{F}[B(\rho_h^k),\mathbf{u}_h^k][\![\phi]\!]d\sigma + \int_{\mathcal{T}_h}\phi\Big(B'(\rho_h^k)\rho_h^k - B(\rho_h^k)\Big)\, div_h\mathbf{u}_h^k dx$$
$$= -\int_{\mathcal{T}_h}\frac{\Delta t}{2}B''(\xi_{\rho,h}^k)\left(\frac{\rho_h^k-\rho_h^{k-1}}{\Delta t}\right)^2\phi dx - h^\alpha\sum_{\Gamma\in\mathcal{E}_{int}}\int_\Gamma \phi\ B''(\overline{\eta}_{\rho,h}^k)[\![\rho_h^k]\!]^2$$
$$-\frac{1}{2}\sum_{\Gamma\in\mathcal{E}_{int}}\int_\Gamma \phi\ B''(\eta_{\rho,h}^k)[\![\rho_h^k]\!]^2|\tilde{\mathbf{u}}_h^k\cdot\mathbf{n}| \quad (19)$$

for any $\phi\in Q_h$, $B\in C^2(0,\infty)$, where $\xi_{\rho,h}^k\in co\{\rho_h^{k-1},\rho_h^k\}$ on each element $K\in\mathcal{T}_h$ and $\eta_{\rho,h}^k,\overline{\eta}_{\rho,h}^k\in co\{\rho_K^k,\rho_L^k\}$ on each face $\Gamma(=K\cap L)\in\mathcal{E}_{int}$.

Lemma 2. *[15, Section 4.2](Renormalized thermal energy)*

$$c_v\int_{\mathcal{T}_h} D_t\left(\rho_h^k\chi(\theta_h^k)\right)\phi - c_v\sum_{\Gamma\in\mathcal{E}_{int}}\int_\Gamma \mathcal{F}(\rho_h^k\chi(\theta_h^k),\mathbf{u}_h^k)\ [\![\phi]\!]d\sigma + \sum_{\Gamma\in\mathcal{E}_{int}}\int_\Gamma\frac{1}{d_\Gamma}[\![\mathcal{K}(\theta_h^k)]\!]\ [\![\chi'(\theta_h^k)\phi]\!]\ \mathrm{dS}_x$$
$$= \int_{\mathcal{T}_h}\Big(2\mu|\mathbf{D}_h(\mathbf{u}_h^k)|^2+\nu|div_h\mathbf{u}_h^k|^2-\rho_h^k\theta_h^k div_h\mathbf{u}_h^k\Big)\chi'(\theta_h^k)\phi - \frac{c_v\Delta t}{2}\int_{\mathcal{T}_h}\chi''(\xi_{\theta,h}^k)\rho_h^{k-1}\left(\frac{\theta_h^k-\theta_h^{k-1}}{\Delta t}\right)^2\phi$$
$$+\frac{c_v}{2}\sum_{\Gamma\in\mathcal{E}_{int}}\int_\Gamma\phi\chi''(\eta_{\theta,h}^k)[\![\theta_h^k]\!]^2(\rho_h^k)^{\mathrm{out}}[\tilde{\mathbf{u}}_h^k\cdot\mathbf{n}]^- - h^\alpha c_v\sum_{\Gamma\in\mathcal{E}_{int}}\int_\Gamma[\![\rho_h^k]\!]\ [\![\Big(\chi(\theta_h^k)-\chi'(\theta_h^k)\theta_k^k\Big)\phi]\!] \quad (20)$$

for any $\phi\in Q_h$, $\chi\in C^2(0,\infty)$, with $\xi_{\theta,h}^k\in co\{\theta_h^{k-1},\theta_h^k\}$ on each element $K\in\mathcal{T}_h$ and $\eta_{\theta,h}^k\in co\{\theta_K^k,\theta_L^k\}$ on each face $\Gamma(=K\cap L)\in\mathcal{E}_{int}$, superscript $'\mathrm{out}'$ denotes the value on the neighbouring element.

By using (19), (20) and the momentum scheme (15a) we deduce similarly as in [15, Section 4.3] the following lemma for the total energy.

Lemma 3 (Total energy balance)**.**

$$D_t\int_{\mathcal{T}_h}\left(\frac{1}{2}\rho_h^k|\widehat{\mathbf{u}}_h^k|^2+c_v\rho_h^k\theta_h^k+\frac{a}{\gamma-1}\left(\rho_h^k\right)^\gamma+b\rho_h^k\log(\rho_h^k)\right)$$
$$+\frac{\Delta t}{2}\int_{\mathcal{T}_h}\left(A\left|\frac{\rho_h^k-\rho_h^{k-1}}{\Delta t}\right|^2+\rho_h^{k-1}\left|\frac{\widehat{\mathbf{u}}_h^k-\widehat{\mathbf{u}}_h^{k-1}}{\Delta t}\right|^2\right)-\sum_{\Gamma\in\mathcal{E}_{int}}\int_\Gamma(\rho_h^k)^{\mathrm{out}}[\tilde{\mathbf{u}}_h^k\cdot\mathbf{n}]^-\frac{\left|\widehat{\mathbf{u}}_h^k-\left(\widehat{\mathbf{u}}_h^k\right)^{\mathrm{out}}\right|^2}{2}$$
$$+\sum_{\Gamma\in\mathcal{E}_{int}}\int_\Gamma\frac{1}{h}[\![\mathbf{u}_h^k]\!]^2+\frac{A}{2}\sum_{\Gamma\in\mathcal{E}_{int}}\int_\Gamma\Big(h^\alpha+|\tilde{\mathbf{u}}_h^k\cdot\mathbf{n}|\Big)[\![\rho_h^k]\!]^2\ \mathrm{dS}_x\le 0 \quad (21)$$

where $A=\min_{\rho>0}\left\{a\gamma\rho^{\gamma-2}+\frac{b}{\rho}\right\}>0$.

3.2 Stability

This subsection is devoted to show the stability by deriving the uniform bounds on the family of numerical solutions independent of the mesh size h.

Mass balance Taking $\phi \equiv 1$ in the continuity scheme (15a) we obtain

$$\int_{\mathcal{T}_h} \rho(t,\cdot)dx = \int_{\mathcal{T}_h} \rho_h^0 dx \approx \int_\Omega \rho^0 dx > 0, \text{ for any } h > 0, \tag{22}$$

which means the total mass is preserved by the scheme.

Uniform bounds The total energy balance (21) gives us the energy bounds

$$\int_{\mathcal{T}_h}\left[\frac{1}{2}\rho_h|\widehat{\mathbf{u}}_h|^2 + c_v\rho_h\theta_h + \frac{a}{\gamma-1}(\rho_h)^\gamma + b\rho_h\log(\rho_h)\right](\tau,\cdot)$$
$$\leq \int_{\mathcal{T}_h}\left[\frac{1}{2}\rho_h^0|\widehat{\mathbf{u}}_h^0|^2 + c_v\rho_h^0\theta_h^0 + \frac{a}{\gamma-1}(\rho_h^0)^\gamma + b\rho_h^0\log(\rho_h^0)\right] \equiv E_h(0),\ E_h(0) \lesssim 1.$$

Further, we deduce the following uniform bounds independent of $h \to 0$ (see [15, Section 5]):

$$\sup_{\tau\in(0,T)}\|\rho_h(\tau,\cdot)\|_{L^\gamma} \lesssim 1, \tag{23a}$$

$$\sum_{\Gamma\in\mathcal{E}_{int}}\int_0^T\int_\Gamma \frac{1}{h}[\![\mathbf{u}_h]\!]^2\, dxdt \lesssim 1. \tag{23b}$$

$$\|\theta_h\|_{L^2(0,T;L^6(\Omega))} + \|\log(\theta_h)\|_{L^2(0,T;L^6(\Omega))} \lesssim 1, \tag{23c}$$

$$\|\theta_h\|_{L^p(0,T;L^q(\Omega))} \lesssim 1 \text{ for any } 1 \leq p < 3,\ 1 \leq q < 9. \tag{23d}$$

Moreover, testing the thermal energy method (15c) with $\phi = 1$, we conclude

$$\int_0^T\int_\Omega |\mathbf{D}_h(\mathbf{u}_h)|^2\, dt \lesssim 1, \tag{23e}$$

together with the second inequality of (23b), and using (14) and (9), we obtain

$$\|\nabla_h\mathbf{u}_h\|^2_{L^2(0,T;L^2(\Omega))} \lesssim 1, \quad \|\mathbf{u}_h\|^2_{L^2(0,T;L^6(\Omega;R^3))} \lesssim 1. \tag{23f}$$

3.3 Consistency

In this section we show the consistency of the scheme (15). The proofs of consistency of the continuity and the temperature equations are the same as in [15, Section 6]. On the other hand, the proof of the consistency of the momentum equation needs more effort on the diffusion terms.

Lemma 4. *[15, Section 6.1](Consistency of continuity) There exists $\beta > 0$, such that for all $\phi \in C^1(\bar{\Omega})$*

$$\int_\Omega [D_t\rho_h - \rho_h\mathbf{u}_h\cdot\nabla_x\phi]\, dx = \int_\Omega R_h^1(t,\cdot)\cdot\nabla_x\phi dx,\ \left\|R_h^1\right\|_{L^2(0,T;L^{\frac{6\gamma}{5\gamma-6}}(\Omega;R^3))} \lesssim h^\beta.$$

Lemma 5 (Consistency of momentum)**.** *There exists $\beta > 0$, such that for all $\mathbf{v} \in C^2(\bar{\Omega})$*

$$\int_\Omega D_t(\rho_h\widehat{\mathbf{u}}_h)\cdot\mathbf{v} - \int_\Omega(\rho_h\widehat{\mathbf{u}}_h\otimes\mathbf{u}_h) : \nabla_x\mathbf{v} + \int_\Omega 2\mu\mathbf{D}_h(\mathbf{u}_h) : \mathbf{D}(\mathbf{v}) + \nu div_h\mathbf{u}_h div_x\mathbf{v}$$
$$- \int_\Omega p(\rho_h,\theta_h)div_x\mathbf{v} = \int_\Omega \mathcal{R}_h^2 : \nabla_x\mathbf{v} + \mathcal{R}_h : \nabla_x^2\mathbf{v},$$

with $\left\|\mathcal{R}_h^2\right\|_{L^1(0,T;L^{\frac{\gamma}{\gamma-1}}(\Omega;R^{3\times3}))} \lesssim h^\beta$ *and* $\|\mathcal{R}_h\|_{L^2(0,T;L^2(\Omega;R^{3\times3}))} \lesssim h^\beta$.

Proof. Here we chose the test function $\Pi_h^V[\mathbf{v}]$ for our scheme. To show the convergence of momentum, it is enough to show

$$\sum_{\Gamma\in\mathcal{E}_{int}}\int_\Gamma \frac{1}{h}[\![u_h]\!][\![\Pi_h^V[\mathbf{v}]]\!] = \int_\Omega \mathcal{R}_h : \nabla_x^2\mathbf{v}, \quad \text{for } \|\mathcal{R}_h\| \lesssim h^\beta, \tag{24}$$

for some constant $\beta > 0$ as the following holds

$$2\mu\int_\Omega \mathbf{D}_h(\mathbf{u}_h) : \mathbf{D}(\Pi_h^V[\mathbf{v}]) = 2\mu\int_\Omega \mathbf{D}_h(\mathbf{u}_h) : \mathbf{D}(\mathbf{v}),$$

by virtue of (7) and the rest part has already been proved in [15, Section 6.2].

Using the fact that $[\![\mathbf{v}]\!] \equiv 0$ together with Hölder's inequality, (8), and (12), we obtain

$$\begin{aligned}\sum_{\Gamma\in\mathcal{E}_{int}}\int_\Gamma \frac{1}{h}[\![u_h]\!][\![\Pi_h^V[\mathbf{v}]]\!] = \sum_{\Gamma\in\mathcal{E}_{int}}\int_\Gamma \frac{1}{h}[\![u_h]\!][\![\Pi_h^V[\mathbf{v}]-\mathbf{v}]\!] &\le \|\mathbf{u}_h\|_{H_V^1(\mathcal{E})}\|\Pi_h^V[\mathbf{v}]-\mathbf{v}\|_{H_V^1(\mathcal{E})} \\ &\lesssim h\|\nabla_h\mathbf{u}_h\|_{L^2}\|\nabla_x^2\mathbf{v}\|_{L^2}.\end{aligned}$$

□

The consistency of temperature is shown through the renormalized equation (20) other than the original scheme (15c), see [15, Section 6.3].

Lemma 6. *[15, Section 6.3](Consistency of temperature)*

$$\begin{aligned}&\int_{\mathcal{T}_h} D_t\left(\rho_h^k\chi(\theta_h^k)\right)\phi - \int_\Omega \rho_h^k\chi(\theta_h^k)\mathbf{u}_h^k\cdot\nabla_x\phi - \int_\Omega \mathcal{K}_\chi(\theta_h^k)\Delta\phi \\ &= \int_\Omega\left(2\mu|\mathbf{D}_h(\mathbf{u}_h^k)|^2 + \nu|div_h\mathbf{u}_h^k|^2\right)\chi'(\theta_h^k)\phi - \int_\Omega \chi'(\theta_h^k)\theta_h^k\rho_h^k div_h\mathbf{u}_h^k\phi + \langle D_h,\phi\rangle + h^\beta\left\langle\mathcal{R}_h^3,\phi\right\rangle,\end{aligned}$$

for some $\beta > 0$, for any $\phi \in C^2(\bar\Omega)$ and $\mathcal{K}_\chi$ is given by $\mathcal{K}_\chi'(\theta) = \chi'(\theta)\mathcal{K}'(\theta)$ and χ belongs to the class $\chi \in W^{2,\infty}[0,\infty)$, $\chi'(\theta) \ge 0$, $\chi''(\theta) \le 0$, $\chi(\theta) = \text{const}$ for all $\theta > \theta_\chi$.

3.4 Convergence

We just briefly list the results that are necessary to prove the convergence. As the vast majority of these results are identical with those presented in [15], we recommend the interested reader to find details of the proofs in there or in references listed therein.

Elastic pressure estimates.

The uniform bound (23a) is not sufficient for passing to the limit in the elastic pressure term, fortunately we can deduce a better integrability of density. To achieve this, one uses the divergence inverse, called Bogovskii operator, that satisfies

$$\mathcal{B}[r] \in W_0^{1,p}(\Omega, R^3), \text{ for } r \in L^p(\Omega), \operatorname{div}_x\mathcal{B}[r] = r, \int_\Omega r\,dx = 0,\ 1 < p < \infty. \tag{25}$$

Then we consider

$$\phi = \mathcal{B}\left[\varrho_h - \frac{1}{|\Omega|}\int_\Omega \varrho_h\,dx\right] \tag{26}$$

in the momentum consistency formulation (5) and shift all terms but the elastic pressure term to the right hand side. Using (25) and our uniform estimates one can show that all these terms are uniformly bounded, which implies

$$\|\varrho_h\|_{L^{\gamma+1}(0,T)\times\Omega} \lesssim 1. \tag{27}$$

Weak sequential compactness, convective and thermal pressure terms.

From the uniform bounds (23a), (23d) and (23f) we deduce that (up to a subsequence)

$$\varrho_h \to \varrho \text{ weakly-* in } L^\infty(0,T;L^\gamma(\Omega)) \tag{28}$$

$$\theta_h \to \theta \text{ weakly in } \ L^p(0,T;L^q(\Omega)), p \in [1,3), q \in [1,9), \tag{29}$$

$$\mathbf{u}_h \to \mathbf{u} \text{ weakly } \text{ in } \ L^2(0,T;L^6(\Omega,R^3)). \tag{30}$$

Next, from (11) and (23f) it follows that $\|\hat{\mathbf{u}}_h - \mathbf{u}_h\|_{L^2(0,T;L^2(\Omega,R^3))} \to 0$, i.e. consequently

$$\hat{\mathbf{u}}_h \to \mathbf{u} \text{ weakly in } L^2(0,T;L^6(\Omega,R^3)), \tag{31}$$

and also

$$\nabla_h \mathbf{u}_h \to \nabla_x \mathbf{u} \text{ weakly in } L^2(0,T;L^2(\Omega,R^{3\times 3})). \tag{32}$$

Moreover, one can deduce from renormalized scheme (19) that $\varrho \geq 0$ (see the detailed proof in a slightly different setting in [22]) and setting $\phi_h \equiv 1$ in (15a) together with the projection of initial condition (17) yield

$$\int_\Omega \varrho(t,.)dx = \int_\Omega \varrho_0 dx, \quad \text{for a.a. } t \in (0,T). \tag{33}$$

A consequence of (23c) is that

$$\theta > 0 \text{ a.e. in } (0,T)\times\Omega. \tag{34}$$

Weak convergences itself do not guarantee convergence of the nonlinear terms in the form of multiplication. These are treated using the discrete version of Aubin–Lions lemma, see [24, Lemma 2.3], in the very same manner as in [15]. We get

$$\varrho_h \mathbf{u}_h \to \varrho\mathbf{u} \text{ weakly in } L^2(0,T;L^{\frac{6\gamma}{\gamma+6}}(\Omega,R^3)), \tag{35}$$

$$\varrho_h \hat{\mathbf{u}}_h \otimes \mathbf{u}_h \to \varrho\mathbf{u}\otimes\mathbf{u} \text{ weakly in } L^q((0,T)\times\Omega,R^{3\times 3}) \text{ for some } q>1, \tag{36}$$

$$\varrho_h \chi(\theta_h) \to \overline{\varrho\chi(\theta)} \text{weakly-* } \text{ in } \ L^\infty(0,T;L^\gamma(\Omega)), \tag{37}$$

$$\varrho_h \chi(\theta_h)\mathbf{u}_h \to \overline{\varrho\chi(\theta)}\mathbf{u} \text{ weakly in } L^2(0,T;L^{\frac{6\gamma}{\gamma+6}}(\Omega,R^3)), \tag{38}$$

where χ is from Lemma 6 and $\overline{f(\varrho,\mathbf{u},\theta)}$ is the limit of $f(\varrho_h,\mathbf{u}_h,\theta_h)$ for $h\to 0$.

In the light of the just listed estimates, one may state the following convergence result for the continuity and momentum scheme:

$$\int_0^T \int_\Omega [\varrho\partial_t\varphi + \varrho\mathbf{u}\cdot\nabla_x\varphi]\,dxdt = -\int_\Omega \varrho_0\varphi(0,.)dx, \tag{39}$$

for any $\varphi \in C_c^1([0,T)\times\Omega)$ and

$$\begin{aligned}\int_0^T \int_\Omega [\varrho\mathbf{u}\cdot\partial_t\varphi + \varrho\mathbf{u}\otimes\mathbf{u} : \nabla_x\varphi + \varrho\theta \mathrm{div}_x\varphi + a\overline{\varrho^\gamma}\mathrm{div}_x\varphi + b\varrho\mathrm{div}_x\varphi]\,dxdt \\ = \int_0^T \int_\Omega [2\mu D_x\mathbf{u} : D_x\varphi + \lambda \mathrm{div}_x\mathbf{u}\mathrm{div}_x\varphi]\,dxdt - \int_\Omega \varrho_0\mathbf{u}_0\cdot\varphi(0,.)dx,\end{aligned} \tag{40}$$

for any $\varphi \in C^2([0,T]\times\Omega)$.

Strong convergence of density.

To show that $\overline{\varrho^\gamma} = \varrho^\gamma$, we need to prove that the sequence of numerical densities converges strongly. This is performed using the so called *effective viscous flux identity*, a technique developed by Lions, see [29].

Roughly speaking, inverse of divergence of the discrete density is as a test function in momentum consistency formulation 5 while the inverse of divergence of the target density is used for testing the equation (40). Comparing these two and using above deduced convergences as well as a convexity argument, one deduces $\varrho_h \to \varrho$ in $L^1((0,T)\times\Omega)$.

For the details of the proof, see [15, Section 7.3], where the only difference when applying the proof to our scheme is the dissipation term that is treated as follows:

$$2\mu\int_\Omega \mathbf{D}_h\mathbf{u}_h : \mathbf{D}_x\mathbf{v}dx = \mu\int_\Omega \mathbf{curl}_h\mathbf{u}_h\cdot\mathbf{curl}_x\mathbf{v}dx + 2\int_\Omega \mathrm{div}_h\mathbf{u}_h\mathrm{div}_x\mathbf{v}dx + 2\langle\mathcal{E},\mathbf{v}\rangle, \tag{41}$$

where

$$\langle\mathcal{E},\mathbf{v}\rangle = \int_\Omega \left(\nabla_h\mathbf{u}_h : \nabla_x^T\mathbf{v} - \mathrm{div}_h\mathbf{u}_h\mathrm{div}_x\mathbf{v}\right)dx = \sum_{E\in E_h}\int_{\partial E}\left(\mathbf{u}_h\cdot\nabla_x\mathbf{v}\cdot\mathbf{n} - \mathbf{u}_h\cdot\mathbf{n}\mathrm{div}_x\mathbf{v}\right)dS_x, \tag{42}$$

compare (41) with [15, equation 7.28]. Notice that $\mathcal{E}$ is the same and thus its treatment can be taken completely from [15]. The first equality of (41) is a consequence of the following observation

$$\begin{aligned} 2\mu\mathbf{D}_h\mathbf{u}_h : \mathbf{D}_x\mathbf{v} &= \mu(\nabla_h\mathbf{u}_h + \nabla_h^T\mathbf{u}_h)(\nabla_h\mathbf{v} + \nabla_x^T\mathbf{v}) = \mu(\nabla_h\mathbf{u}_h : \nabla_x\mathbf{v} + 2\mu\nabla_h\mathbf{u}_h : \nabla_x^T\mathbf{v}) \\ &= \mu\nabla_h\mathbf{u}_h : (\nabla_x\mathbf{v} - \nabla_x^T\mathbf{v}) + 2\mu\nabla_h\mathbf{u}_h : \nabla_x^T\mathbf{v} = \mu\mathbf{curl}_h\mathbf{u}_h\cdot\mathbf{curl}_x\mathbf{v} + 2\mu\nabla_h\mathbf{u}_h : \nabla_x^T\mathbf{v}. \end{aligned} \tag{43}$$

Convergence of the temperature.

The last step of the proof is establishing strong (almost everywhere) pointwise convergence of the density. This is performed in the very same way as in [15, Section 7.4] and is therefore omitted.

4 Numerical experiments

To illustrate the performance of the schemes, we present two numerical experiments in 2D, with the aim to show the numerical convergence rate and positivity of density. Due to the implicit time discretization, we have no stability condition between a time step and a spatial mesh parameter. On the other hand, we solve the nonlinear systems by fixed point iteration method and we have to control the inner time substeps at each time step. Alternatively, one can use the (quasi-)Newton method, which will relax the time step restriction.

4.1 Experiment 1

In this experiment we aim to show the convergence and accuracy of the schemes by a plane Poiseulle flow

$$\mathbf{u} = \big(U,0\big)^T,\ \rho = 1 + \frac{1}{2}\sin\big(2\pi(x-Ut)\big),\ \theta = 1 + \frac{1}{2}\sin(2\pi t)\cos^2(2\pi x)\cos^2(2\pi y),$$

with $U = y(1-y)$. The parameters are chosen in agreement with the assumptions in Section 1 by $a = b = c_v = \mu = 1$, $\lambda = \mu/3$, $\gamma = 4$, $\alpha = 0.83$, $\kappa(\theta) = 1+\theta^2$. For the boundary

Table 1: Error norms and EOC.

h	$\|\rho\|_{L^\infty(L^\gamma)}$	EOC	$\|\rho\|_{L^1(L^1)}$	EOC	$\|\mathbf{u}\|_{L^2(L^2)}$	EOC	$\|\nabla\mathbf{u}\|_{L^2(L^2)}$	EOC	$\|\theta\|_{L^2(L^6)}$	EOC
1/32	2.31e-02	–	1.16e-02	–	3.27e-02	–	1.59e-01	–	3.63e-02	–
1/64	1.06e-02	1.12	5.04e-03	1.20	1.34e-02	1.29	7.95e-02	1.00	1.38e-02	1.40
1/128	5.10e-03	1.06	2.40e-03	1.07	5.87e-03	1.19	4.14e-02	0.94	5.61e-03	1.30
1/256	2.62e-03	0.96	1.25e-03	0.94	2.70e-03	1.12	2.22e-02	0.90	2.43e-03	1.21

(a) Scheme-SA.

h	$\|\rho\|_{L^\infty(L^\gamma)}$	EOC	$\|\rho\|_{L^1(L^1)}$	EOC	$\|\mathbf{u}\|_{L^2(L^2)}$	EOC	$\|\nabla\mathbf{u}\|_{L^2(L^2)}$	EOC	$\|\theta\|_{L^2(L^6)}$	EOC
1/32	2.40e-02	–	1.25e-02	–	3.47e-02	–	4.10e-01	–	5.34e-02	–
1/64	1.08e-02	1.15	5.25e-03	1.25	1.38e-02	1.33	2.06e-01	0.99	1.65e-02	1.69
1/128	5.16e-03	1.07	2.45e-03	1.10	5.96e-03	1.21	1.04e-01	0.99	5.86e-03	1.49
1/256	2.63e-03	0.97	1.26e-03	0.96	2.72e-03	1.13	5.24e-02	0.99	2.42e-03	1.28

(b) Scheme-SB.

conditions we have no-slip insulated wall on the top and bottom boundaries while periodic in horizontal direction. Table 1 presents the convergence results of the numerical solution to the exact solution and these results are further presented in Figure 1. Clearly, the numerical results support our main result Theorem 1. Moreover, the two schemes perform similar behaviour of convergence.

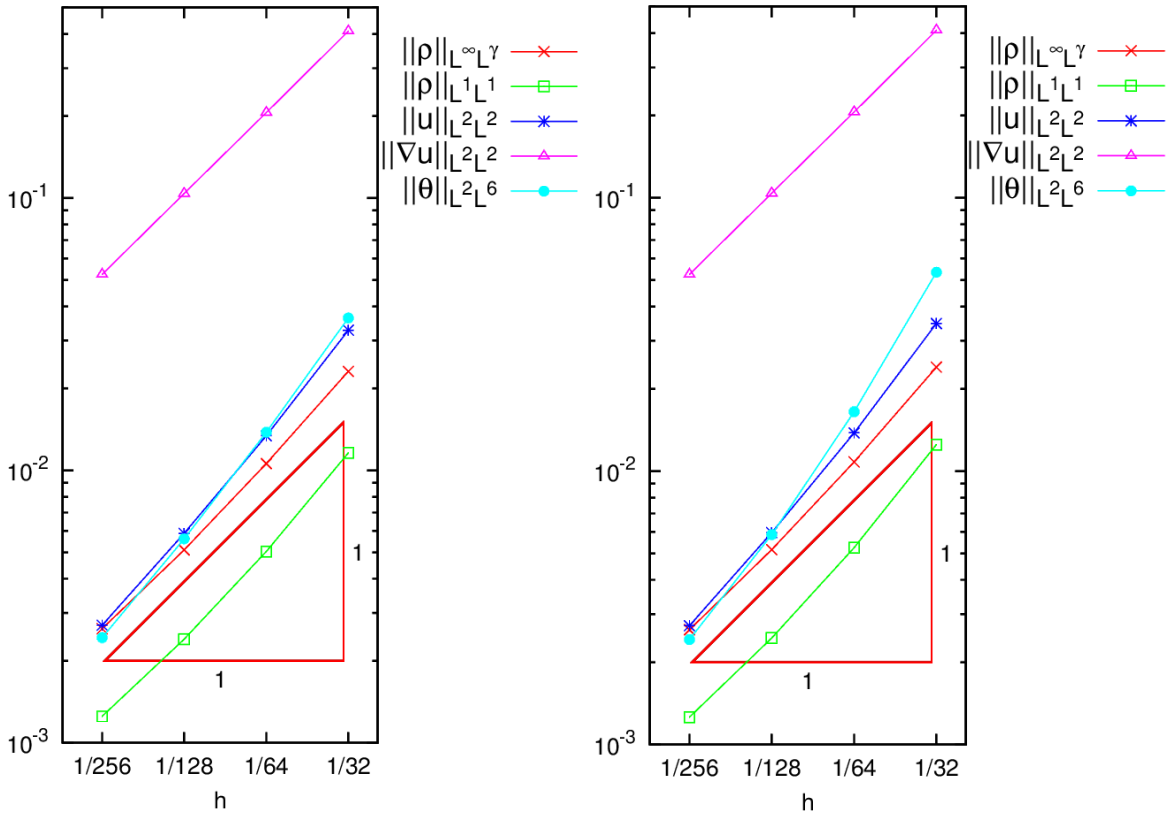

(a) Scheme-SA (b) Scheme-SB

Figure 1: Relative errors of the numerical test

4.2 Experiment 2

This experiment is a benchmark Riemann problem for checking the positivity preserving of the scheme. The initial values are setting as

$$(\rho, u_1, u_2, p) = \begin{cases} (1, -2, 0, 0.4) & \text{if } x \leq 0.5, \\ (1, 2, 0, 0.4) & else. \end{cases}$$

We have chosen the equation of state of a perfect gas $p = \rho\theta$ with $\gamma = 1.4$, $c_v = 2.5$, $\mu = 5\times10^{-4}$, $\lambda = \mu/3$, $\kappa(\theta) = a = b = 0$, $\alpha = 0.83$. In this case, there are two rarefaction waves travelling away from the center $x = 0.5$. Consequently, a vacuum area is generated. Then it is crucial to preserve the positivity for the density approximated by the numerical scheme. We show in Figure 2 the density ρ, pressure p, internal energy Θ, and velocity component u_1 at time $t = 0.15$ for both schemes. Clearly the two schemes show similar behaviour and the numerical positivity is well preserved.

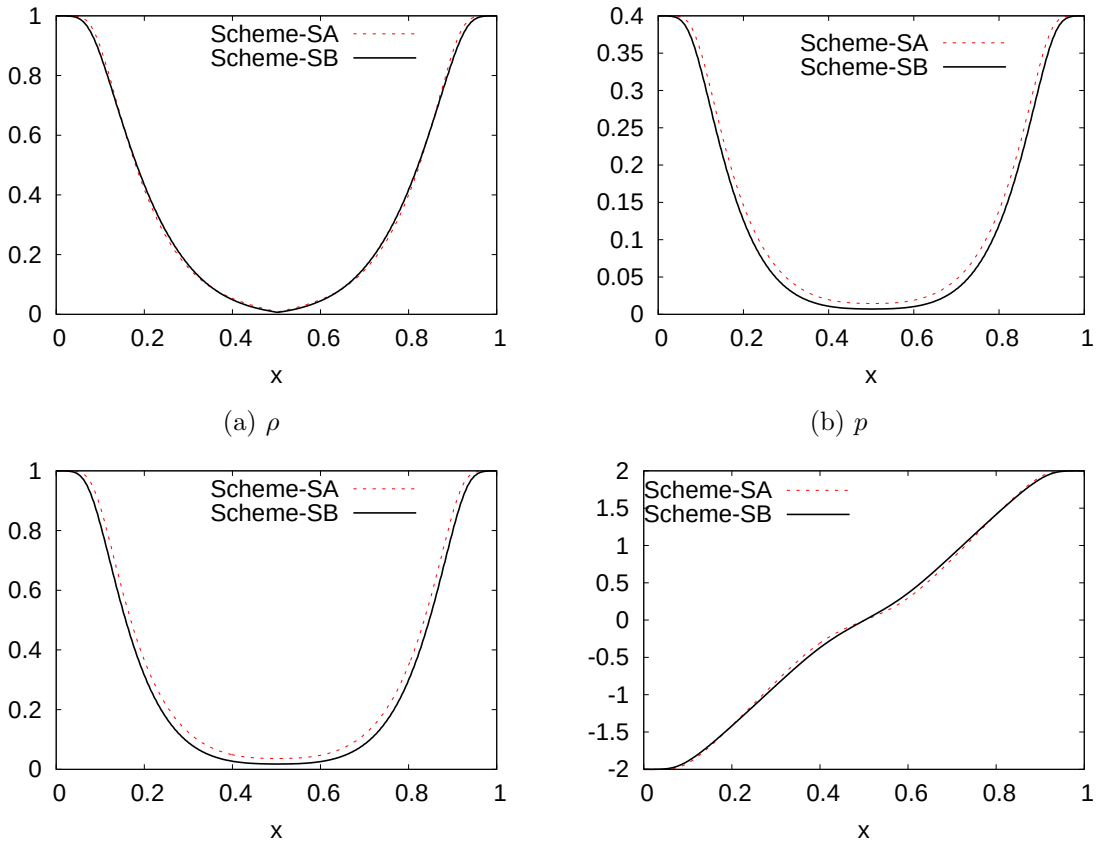

(a) ρ (b) p

(c) Θ (d) u_1

Figure 2: result of Experiment 1 at time $t = 0.15$.

Acknowledgement. The authors would like to thank Prof. E. Feireisl (Czech Academy of Sciences, Prague) for fruitful discussions and suggestions. B.S. would like to thank Dr. H. Shen (King Abdullah University of Science and Technology, Thuwal) for the computational power.

References

[1] S. C. Brenner, *Poincaré–Friedrichs inequalities for piecewise H1 functions*, SIAM J. Numer. Anal., 41 (2003), pp. 306–324.

[2] S. C. Brenner, *Korn's inequalities for piecewise H1 vector fields*, Mathematics of Computation, (2004), pp. 1067–1087.

[3] E. Burman and P. Hansbo, *Stabilized Crouzeix-Raviart element for the Darcy-Stokes problem*, Numer. Methods Partial Differential Equations, 21 (2005), pp. 986–997.

[4] C. Chainais-Hillairet and J. Droniou, *Finite-volume schemes for noncoercive elliptic problems with Neumann boundary conditions*, IMA J. Numer. Anal., 31 (2011), pp. 61–85.

[5] Z. J. Chen and A. J. Przekwas, *A coupled pressure-based computational method for incompressible/compressible flows*, J. Comput. Phys., 229 (2010), pp. 9150–9165.

[6] P. I. Crumpton, J. A. Mackenzie, and K. W. Morton, *Cell vertex algorithms for the compressible Navier-Stokes equations*, J. Comput. Phys., 109 (1993), pp. 1–15.

[7] V. Dolejší and M. Feistauer, *Discontinuous Galerkin method*, vol. 48 of Springer Series in Computational Mathematics, Springer, Cham, 2015. Analysis and applications to compressible flow.

[8] R. Eymard, T. Gallouët, and R. Herbin, *Convergence of finite volume schemes for semilinear convection diffusion equations*, Numer. Math., 82 (1999), pp. 91–116.

[9] R. Eymard, T. Gallouët, R. Herbin, and A. Michel, *Convergence of a finite volume scheme for nonlinear degenerate parabolic equations*, Numer. Math., 92 (2002), pp. 41–82.

[10] E. Feireisl, *Dynamics of viscous compressible fluids*, vol. 26 of Oxford Lecture Series in Mathematics and its Applications, Oxford University Press, Oxford, 2004.

[11] E. Feireisl, *The Navier-Stokes-Fourier system: from weak solutions to numerical analysis.*, Analysis, München, 35 (2015), pp. 185–193.

[12] E. Feireisl, R. Hošek, D. Maltese, and A. Novotný, *Error estimates for a numerical method for the compressible Navier-Stokes system on sufficiently smooth domains*, ESAIM: M2AN, 51 (2017), pp. 279–319.

[13] E. Feireisl, R. Hošek, and M. Michálek, *A convergent numerical method for the full Navier–Stokes–Fourier system in smooth physical domains*, SIAM J. Numer. Anal., 54 (2016), pp. 3062–3082.

[14] E. Feireisl, T. Karper, and M. Michálek, *Convergence of a numerical method for the compressible Navier-Stokes system on general domains*, Numer. Math., (2015), pp. 1–38.

[15] E. Feireisl, T. Karper, and A. Novotný, *A convergent numerical method for the Navier–Stokes–Fourier system*, IMA J. Numer. Anal., 36 (2016), pp. 1477–1535.

[16] E. Feireisl and A. Novotný, *Weak-strong uniqueness property for the full Navier-Stokes-Fourier system*, Arch. Ration. Mech. Anal., 204 (2012), pp. 683–706.

[17] M.-f. Feng, R.-s. Qi, R. Zhu, and B.-t. Ju, *Stabilized Crouzeix-Raviart element for the coupled Stokes and Darcy problem*, Appl. Math. Mech. (English Ed.), 31 (2010), pp. 393–404.

[18] T. Gallouët, R. Herbin, and J.-C. Latché, *A convergent finite element-finite colume scheme for the compressible Stokes problem. I. The isothermal case.*, Math. Comput., 78 (2009), pp. 1333–1352.

[19] B. Gao, S.-S. Xu, and Z.-N. Wu, *A note on hybrid Eulerian/Lagrangian computation of compressible inviscid and viscous flows.*, J. Comput. Phys., 226 (2007), pp. 1–16.

[20] F. Grasso and C. Meola, *Euler and Navier-Stokes equations for compressible flows: finite-volume methods*, in Handbook of computational fluid mechanics, Academic Press, San Diego, CA, 1996, pp. 159–282.

[21] P. Hansbo and M. G. Larson, *Discontinuous Galerkin and the Crouzeix-Raviart element: application to elasticity*, ESAIM: M2AN, 37 (2003), pp. 63–72.

[22] R. Hošek and B. She, *Stability and consistency of a finite difference scheme for compressible viscous isentropic flow in multi-dimension*, Accepted to J. Numer. Math., (2017).

[23] C. S. Jog, *A finite element method for compressible viscous fluid flows*, Int. J. Numer. Methods Fluids, 66 (2011), pp. 852–874.

[24] K. H. Karlsen and T. K. Karper, *A convergent mixed method for the Stokes approximation of viscous compressible flow*, IMA J. Numer. Anal., 32 (2012), p. 725.

[25] T. K. Karper, *A convergent FEM-DG method for the compressible Navier-Stokes equations*, Numer. Math., 125 (2013), pp. 441–510.

[26] C. M. Klaij, J. J. W. van der Vegt, and H. van der Ven, *Space-time discontinuous Galerkin method for the compressible Navier-Stokes equations*, J. Comput. Phys., 217 (2006), pp. 589–611.

[27] M. Kouhi and E. Oñate, *An implicit stabilized finite element method for the compressible Navier-Stokes equations using finite calculus*, Comput. Mech., 56 (2015), pp. 113–129.

[28] M. Kupiainen and B. Sjögreen, *A Cartesian embedded boundary method for the compressible Navier-Stokes equations*, J. Sci. Comput., 41 (2009), pp. 94–117.

[29] P.-L. Lions, *Mathematical topics in fluid mechanics. Vol. 2: Compressible models.*, Oxford: Clarendon Press, 1998.

[30] J. S. Park and C. Kim, *Higher-order multi-dimensional limiting strategy for discontinuous Galerkin methods in compressible inviscid and viscous flows*, Comput. & Fluids, 96 (2014), pp. 377–396.

[31] F. Renac, S. Gérald, C. Marmignon, and F. Coquel, *Fast time implicit-explicit discontinuous Galerkin method for the compressible Navier-Stokes equations*, J. Comput. Phys., 251 (2013), pp. 272–291.

[32] H. Shen, C.-Y. Wen, and D.-L. Zhang, *A characteristic space-time conservation element and solution element method for conservation laws.*, J. Comput. Phys., 288 (2015), pp. 101–118.

[33] E. Vanderzee, A. N. Hirani, D. Guoy, and E. A. Ramos, *Well-centered triangulation*, SIAM J. Sci. Comput., 31 (2009/10), pp. 4497–4523.

[34] E. VanderZee, A. N. Hirani, D. Guoy, V. Zharnitsky, and E. A. Ramos, *Geometric and combinatorial properties of well-centered triangulations in three and higher dimensions*, Comput. Geom., 46 (2013), pp. 700–724.

[35] L. Wang, W. K. Anderson, J. T. Erwin, and S. Kapadia, *Discontinuous Galerkin and Petrov Galerkin methods for compressible viscous flows*, Comput. & Fluids, 100 (2014), pp. 13–29.

[36] K. Xu, C. Kim, L. Martinelli, and A. Jameson, *BGK-based schemes for the simulation of compressible flow.*, Int. J. Comput. Fluid Dyn., 7 (1996), pp. 213–235.